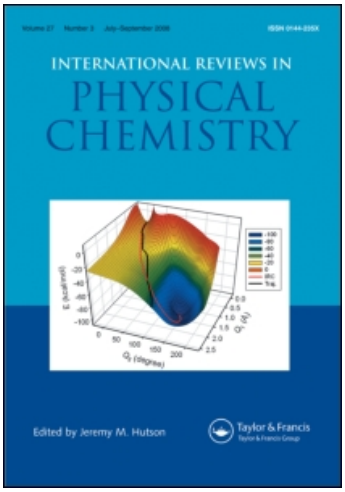

International Reviews in Physical Chemistry
Publication details, including instructions for authors and subscription information:
http://www.informaworld.com/smpp/title~content=t713724383

Reactions of oxygen atoms with van der Waals molecules in crossed molecular beams

Anne B. Mccoy; Ron Naaman

Online publication date: 26 November 2010

To cite this Article Mccoy, Anne B. and Naaman, Ron(1999) 'Reactions of oxygen atoms with van der Waals molecules in crossed molecular beams', International Reviews in Physical Chemistry, 18: 4, 459 — 484
To link to this Article: DOI: 10.1080/014423599229893
URL: http://dx.doi.org/10.1080/014423599229893

INT. REVIEWS IN PHYSICAL CHEMISTRY, 1999, VOL. 18, NO. 4, 459–484

Reactions of oxygen atoms with van der Waals molecules in crossed molecular beams

ANNE B. McCOY
Department of Chemistry, The Ohio State University, Columbus, OH 43210, USA

and RON NAAMAN
Department of Chemical Physics, Weizmann Institute, Rehovot 76100, Israel

Studies of reactions of van der Waals (vdW) molecules or clusters can provide a window through which we can investigate a variety of effects of weak intermolecular interactions on the chemical process of interest. Here we focus on the reactions of oxygen atoms with vdW complexes. These reactions were chosen since the reactions of oxygen atoms with hydrogen halides, saturated hydrocarbons and water molecules have been studied extensively in both the gas and the condensed phases. In addition, the presence of a low-lying excited electronic state, in the oxygen atom, means that its chemistry may be particularly sensitive to perturbations of the environment, for example those introduced by incorporating one or more of the reactants into a vdW complex. In this review we discuss association reactions of oxygen atoms with CO and NO and the reactions of oxygen atoms, both in their ground $O(^3P)$ state and in the excited $O(^1D)$ state, with saturated hydrocarbons, water and with HCl complexes. The studies of the reactions of oxygen atoms with vdW molecules were used to gain insights into generic effects of complex formation on chemical reaction dynamics, reactivity and product state distributions. The results of these studies were summarized in several general rules that describe the effects of the 'environment' on bimolecular reactions.

Contents

International Reviews in Physical Chemistry ISSN 0144-235X print/ISSN 1366-591X online © 1999 Taylor & Francis Ltd
http://www.tandf.co.uk/JNLS/rpc.htm http://www.taylorandfrancis.com/JNLS/rpc.htm

1. Introduction

In the process of transferring knowledge and intuition from gas- to condensed-phase processes, one is faced with the question of how the environment affects chemical processes. For example, one can ask whether changes in the environment will lead to the emergence of properties that were not observed in the isolated gas-phase process. In the discussion that follows, we shall use the term 'environment' to represent the solvent or other molecules that interact weakly with the reactants and products of the reaction of interest. Studies of reactions of van der Waals (vdW) molecules or clusters can provide a window through which we can investigate a variety of effects of weak intermolecular interactions on the chemical process of interest. These issues have been the subjects of numerous studies [1–5] and review articles in recent years [6–13]. In the discussion that follows, we shall focus on the reactions of oxygen atoms with a variety of vdW molecules and clusters. The chemistry of reactions with atomic oxygen is of interest because of the importance of oxygen in many common chemical processes in solution, in biological systems and in important atmospheric processes [14]. In addition, the presence of low-lying excited electronic states means that the chemistry of oxygen atoms may be particularly sensitive to perturbations of the environment, for example those introduced by incorporating one or more of the reactants into a vdW complex. We shall try to use our studies of the reactions of oxygen atoms with vdW molecules to gain insights into generic effects of complex formation on chemical reaction dynamics, reactivity and product state distributions. When possible, we shall use the results of these studies to develop general rules that describe the effects of the 'environment' on bimolecular reactions.

The reactions of oxygen atoms with hydrogen halides, saturated hydrocarbons and water molecules have been studied extensively in both the gas and the condensed phases (for several recent studies on the reactions of oxygen atoms see [15]). Owing to the amount of very detailed information about reaction dynamics that can be obtained from gas-phase studies, these studies have provided a vast amount of information about the chemistry of these processes. The motivation for performing detailed studies of the chemistry of isolated vdW molecules comes from the notion that insights that are gained from these studies will be relevant to 'real-life' chemistry, specifically chemistry occurring in solution or on surfaces. The notion that mechanisms inferred from studies of isolated molecules can be transferred to processes occurring in condensed media is based on the assumption that solvent–solute interactions are small compared with the separations between electronic states. This assumption is well justified when regions of the potentials that are near crossings of two or more electronic states are not energetically accessible. However, it is well known that the potential energy surfaces for reactions of atomic oxygen cross because of symmetry breaking and spin–orbit couplings. Therefore, it is likely that the reactions mechanisms, inferred from gas-phase studies, will be strongly affected by small changes to the environment.

vdW molecules and clusters provide a laboratory in which the effects of solvation on chemical reaction dynamics can be investigated. They have the advantage that most

of the experimental tools that have been developed for studying gas-phase reactions can be applied to these investigations. In addition, the relative ease with which computer simulations can be performed on the vdW systems, since their size and the initial conditions are both well defined, make these systems ideal for theoretical and computational studies. Finally, as we shall demonstrate below, in many cases the presence of a small number of solvent molecules can lead to the solvent effects that are similar to those observed in liquids.

Studies of reactions of neutral vdW molecules can be performed in one of two configurations. In the first, a vdW complex is produced and the reaction inside the cluster is initiated by dissociating or by electronically exciting one of the components in the complex. This type of study was reviewed recently [8–12], and we shall refer to these reactions as intracluster processes. The second type of study is performed in a crossed-molecular-beam set-up. Here a beam of complexes is intersected by a beam of reacting atoms or molecules. These intercluster reactions will be the focus of the present review.

2. The kinematics, kinetics and electronic effects

When reactions of two isolated species take place, there are severe constraints on the chemistry. The most obvious of these are the conservation of energy and linear and angular momenta. When relatively small molecules are involved, the lifetime of the collision complex is short. Attaching a 'third body' to the reactants, even a single atom, can relax the above constraints on the reacting species and significantly lengthen the collision complex lifetime.

In the discussion that follows, we shall focus on three types of effects that are expected to result from complex formation: kinematics, kinetics and electronic. We shall illustrate these effects using the results of classical trajectory calculations, performed on a London–Eyring–Polyani–Sato (LEPS) potential that represents the $O(^3P) + HR$ reaction. Here R is approximated by a single unified fragment, which represents the rest of the hydrocarbon molecule. The simulations are also performed [16] with an argon atom attached in an R–H–Ar geometry.

One may argue that, owing to the weak interactions between the spectator atom and the reactants, it is expected that this 'third body' will leave the collision complex first. In fact, as can be seen in the results plotted in figure 1, in general this is not the case for the generic $O(^3P) + Ar{\bullet}HR$ reaction. Owing to the weak interactions between the argon atom and the other species in the system, there is a long delay between the time when the force is exerted on the vdW bond and when the spectator feels the impact. Consequently, the vdW complex will often be longer lived than the collision complex.

It is important to realize that classical trajectory simulations may easily miss the magnitude of this effect. This is a consequence of the differences between the probability distributions for molecular vibrations obtained from classical and quantum treatments, plotted in figure 2. These differences can have a dramatic effect on the calculated lifetime of a vdW complex after collision with oxygen. The reason for this can be understood as follows. In classical mechanics, the intermolecular modes are primarily sampling regions of the potential near the turning points, where the gradient is largest. When a collision occurs, there will be a sharp change in the potential energy in the vdW modes. By contrast, in quantum mechanics or when classical simulations are biased by a quantum-mechanical distribution [17], the most probable configuration

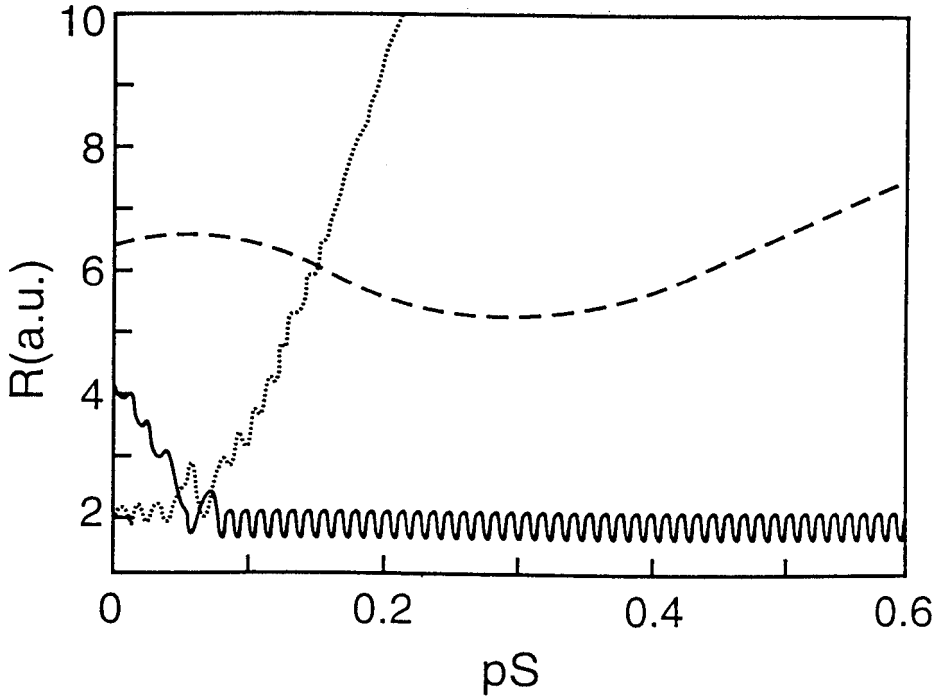

Figure 1. Time dependences of the OH (——), RH (-----) and RAr (– – –) distances from a representative trajectory for the $O(^3P) + Ar \bullet HR$ reaction. (Reprinted, with permission, from [16].)

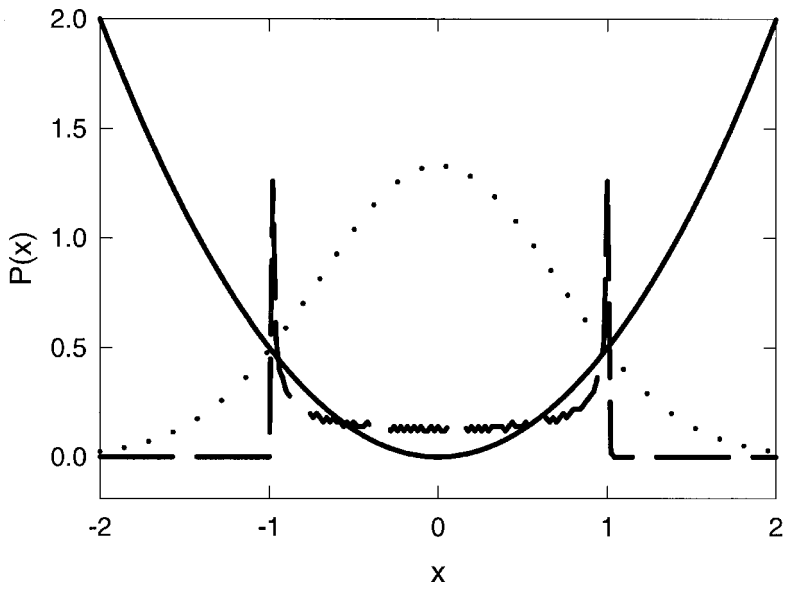

Figure 2. A comparison of the quantum (– –) and classical (· · · ·) probability distributions for the ground state of a harmonic oscillator potential (——).

of the vdW modes is at the minimum-energy geometry, where the gradient of the potential is zero. In this case, the collision with oxygen will lead to a much smaller change in the potential energy in these coordinates. By comparing the quantum and classical dynamics, it becomes clear that the energy transfer into the vdW coordinates will be more efficient in classical simulations than in quantum-mechanical simulations. Since energy transfer is less efficient in the quantum case, we anticipate that the lifetimes obtained from classical simulations could be significantly shorter than those obtained from quantum simulations. Preliminary studies of the effect of initial conditions on the calculated collision complex lifetime support this idea [18].

2.1. *The kinematics effect*

Constraints due to linear and angular momenta do not usually affect the observed products or their internal energy distributions. However, the conservation of both energy and angular momentum can have a major impact on the way that energy is distributed among the products. The role of the third body in terms of energy uptake is relatively straightforward and usually not particularly important. This is due to the weak coupling between the internal degrees of freedom of the reactants and those of the spectator atoms or molecules. The small size of this coupling is also the reason why only a small fraction of the collision energy is expressed in the inert species.

However, the kinematic effect is very profound in association and exchange reactions. Worsnop *et al.* [1(b)] observed that kinematics play a major role in exchange reactions involving vdW complexes. In addition, the association reactions of $O(^3P)$ with CO [19] and with NO [20, 21] are dramatically enhanced by the introduction of the 'third body'.

A general trend that is observed in almost all reactions of vdW complexes is the rotational 'cooling' of the products, compared with that observed for the corresponding monomeric processes. This decrease in energy in the rotational degrees of freedom can be rationalized by the availability of more states that conserve the total angular momentum when the reaction occurs in a complex. However, in some cases the rotational energy in one of the products is even lower than predicted by the statistical arguments. The explanation for this effect lies in the facts that the observed fragment is a diatomic and the collision complex is long lived. In this case, the energy distribution of the diatomic product can be described by a model that is similar to that which is used to explain the low rotational population in diatomic products desorbed from surfaces [22] or in diatomic products probed following infrared multiphoton dissociation [23]. Another explanation for the observed rotational cooling is rotational energy exchange. Interacting rotors can end up with much less rotational energy they had initially owing to rotational to translational energy transfer.

2.2. *The kinetics effect: kinetics versus thermodynamics*

Reactions in crossed molecular beams are usually controlled by the kinetics of the reaction and not its thermodynamics. By lengthening the lifetime of the collision complex, the system will have enough time to find a low-energy path and follow the thermodynamics. Since this effect is related to the increases in the collision complex lifetime, it is closely associated with the kinematics. For example, the existence of a spectator allows the system to explore regions of phase space that are not available to the isolated system. By exploring larger regions of phase space, it becomes more probable that the system will find a way to bypass high-energy barriers.

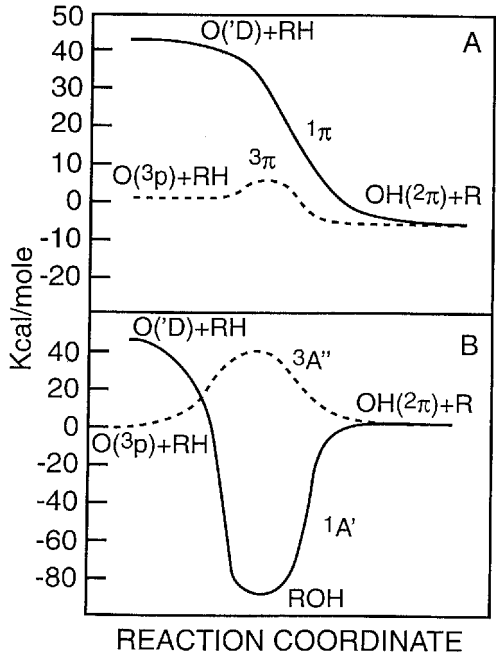

Figure 3. A schematic representation of the potential energy surfaces related to the reaction of atomic oxygen with saturated hydrocarbons (*a*) in a collinear configuration and (*b*) when the oxygen atom is approaching at a 90° angle relative to the C–H bond. (Reprinted, with permission, from [24].)

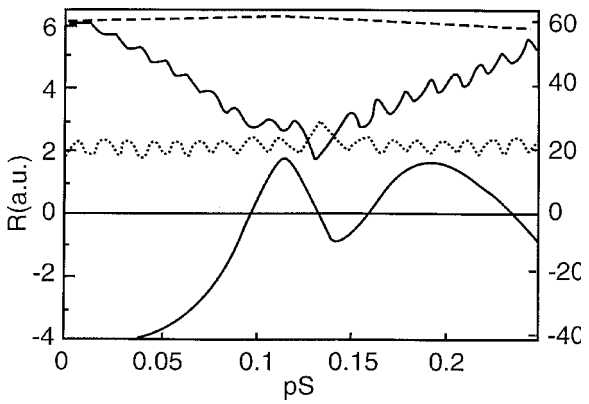

Figure 4. Bending motion in a reactive O + Ar•HR trajectory. In addition to the bending angle θ (lower ——), the R–H (···), O–H (upper ——) and Ar–R (– – –) distances are also shown. (Reprinted, with permission, from [16].)

We shall refer again to the O(^{3}P) + HR reaction. As shown in figure 3, in the collinear configuration there is a barrier on the triplet surface. However, if the oxygen atom approaches in a collinear configuration and then samples the T-shaped geometry, it has a chance to cross down to the singlet surface and to insert into the HR bond instead of abstracting the hydrogen atom. An example of a trajectory that could undergo such a transition is shown in figure 4. Clearly, this system undergoes many bending vibrations during the lifetime of the collision complex. This is the motion that

is required to induce efficient crossing between the triplet and singlet surfaces. Similar results have also been obtained in simulations of the liquid-phase processes [25].

2.3. *The electronic effect: ionization potentials, electron affinity and electronic state mixing*

Perhaps the most dramatic of the effects that are expected to result from the formation of vdW complexes are electronic in nature. These effects are usually unexpected, since electronic energy differences are typically much larger than those related to the vdW interaction. It is important to realize that relative energies may not provide a particularly sensitive indicator for mixing of electronic states. Since reactions are related to the electronic wavefunctions, minute changes to the wave function, that have little effect on the eigenvalues, can have a large effect on the reactivity. This effect can be particularly pronounced in cases of symmetry-forbidden processes, where the reactivity of the monomers is extremely low. The addition of a spectator can break the symmetry and open previously closed channels. Because there is zero background from the monomeric process, these processes are relatively easy to probe. This type of phenomenon was first suggested by Dixon *et al.* [1(a)] in changing a four-centre forbidden process into a six-centre allowed reaction.

Another type of electronic effect has been observed in the $Ba + CO_2$ reaction [26]. There it was found that formation of CO_2 dimers increased the reaction cross-section by nearly an order of magnitude. This observation was explained by a change in the mechanism from a direct to a harpooning process. The change in mechanism can be rationalized in terms of the dramatic change in the electron affinity of CO_2 brought about by cluster formation. A more general electronic phenomenon comes from the crossing of two potential surfaces, induced by the complex formation. This phenomenon will be discussed in details in the case of the reaction of $O(^1D)$ with hydrocarbons.

3. The complex size effect: methane, propane and water clusters

In discussing the effect of complex size on reactions of neutral vdW complexes and clusters, one has to realize that very few truly size-dependent experimental studies have been performed. This is due to the difficulty in separating or distinguishing between clusters of different sizes that are produced in molecular beams. Several methods for discriminating between clusters of various sizes have been developed. These include the elegant method of Buck and Ettischer [3] that exploits the fact that neutral clusters of different masses will be scattered at different angles upon collision with a beam of He atoms. Alternatively, laser-induced reaction enhancement processes have been employed. In this approach, a photon, usually in the infrared, is used to enhance the reactivity of a size-selected complex. This method has been primarily used in studies of photodissociation processes in clusters (for example [27, 28]). In all, very few systems have been studied using either of these techniques. Therefore, most of the available information on size-dependent reactivity is based on indirect evidence, including the conditions in the molecular beam or by using ionization or spectroscopic methods to analyse the cluster size distribution in the molecular beam.

Clearly, as the size of the clusters increases, the system will contain more degrees of freedom. One may expect that this will cause the reaction to behave more 'statistically' as the cluster size increases. As will be shown, this view represents an oversimplification of the cluster 'size' effects that are important in reactions of atomic species with a complex. We have found that there are three general situations.

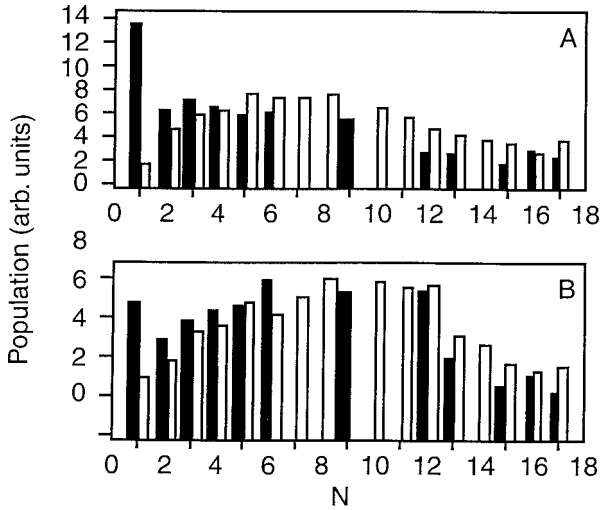

Figure 5. Rotational energy distributions for the $^2\Pi_{3/2}$ (black bars) and $^2\Pi_{1/2}$ (white bars) spin orbit states of OH produced from the reaction of $O(^1D)$ with (*a*) H_2O and $(H_2O)_2$ and with (*b*) $(H_2O)_n$, $2 < n < 6$. The estimated error in these results is approximately 10%.

In the first, the monomers that make up the cluster are themselves 'large molecules', containing a sufficient number of vibrational degrees of freedom that the monomeric reaction behaves statistically. In this case, cluster formation is expected to have no effect on the reaction. This is the case for the reaction of $O(^1D)$ with propane, where increasing the size of the propane clusters has no observable effect on the internal energy of the OH product [29, 30].

A second class of systems includes those in which the units that make up the cluster are held together by weak vdW interactions. In this case, one expects that there will be differences between reactions of clusters and the monomeric species since the existence of a 'third body' will affect the kinematics of the reaction. However, since the molecules in the complex are weakly coupled, energy is not easily transferred between the units and the size effect is expected to be small. This type of behaviour was observed in the reaction of $O(^1D)$ with methane clusters, where clusters react to form OH that is rotationally cold, compared with the monomeric process, a result that is independent of the size of the cluster [29].

The third class of systems includes those in which the constituents are strongly coupled, as is the case in water complexes. Here, one expects to observe a size effect on the observed products and on their internal energy distributions. This type of behaviour is exemplified by the reaction of $O(^1D)$ with water clusters, shown in figure 5. In this reaction, three size regimes are observed. For small clusters, dimers and perhaps trimers, the OH product is produced with less internal energy than is expressed in the OH products obtained from the monomeric process. For medium-sized clusters, with up to seven or eight water molecules, a statistical internal energy distribution is observed, while reactions with larger clusters do not produce any OH products. These results can be understood in terms of the distribution of energy among the water subunits. When the complex is small, cooling by means of rotational to translational energy transfer is observed. This behaviour is qualitatively similar to that observed for reactions of weakly bound complexes, described above. When the size of the cluster increases, the collision complex lifetime increases and the system behaves

statistically. However, for large complexes, containing more than eight water subunits, the lifetime of the complex after reaction provides sufficient time for the OH products to recombine on the surface of the complex. Consequently, no free OH is detected [30].

4. Internal energy distributions in the products

When discussing the internal energy distributions of the OH products, formed by reactions of atomic oxygen with clusters containing saturated hydrocarbons, HCl and water there are three effects that should be considered. They are the vibrational energy and angular momentum distributions as well as the relative populations of the $^2\Pi_{1/2}$ and $^2\Pi_{3/2}$ spin–orbit states of the OH formed by the reaction. We shall consider these in order from highest- to lowest-energy effects.

In the case of vibrational energy, both experiment and classical trajectory simulations indicate a decrease in population of the $v = 1$ state of OH when the reaction occurs in a cluster. In the case of reactions of $O(^1D)$ with methane and methane clusters, the ratio of the population in $v = 1$ to the population in $v = 0$ decreases from 1.22 to 0.20 when clusters of methane were reacted [29]. The vibrational distributions resulting from reactions of $O(^3P)$ with HCl and Ar•HCl at 1 eV collision energies are plotted in figure 6(*a*). In this case, the relative populations in the $v = 1$ and $v = 0$ states of OH decrease from 0.255 to 0.056 when a single argon atom is introduced [31]. The main reason for the observed decrease in the population on vibrationally excited states of OH comes from the fact that the non-reactive species in the cluster will take with them a fraction of the collision energy. In the case of the $O(^3P)$ + HCl reaction, this corresponds to approximately 10% of the collision energy. A second mechanism for the loss of vibrational energy comes from the fact that in these systems the collision complex is shorter lived than the vdW complex.

This second effect, while possibly important in the mechanism for the decrease in vibrational energy expressed in the OH product, will definitely play a role in the observed rotational cooling of the OH product after reaction. This effect is clearly illustrated in figure 7, in which we have plotted the angular momentum distributions for the two spin–orbit states of OH when $O(^1D)$ reacts with methane and clusters. Similar effects can be seen in classical studies of the reaction of $O(^3P)$ with HCl and Ar•HCl. In figure 6(*b*), we plot the rotational distributions that correspond to the vibrational distribution plotted in figure 6(*a*). To simplify the comparison, instead of plotting the full angular momentum distributions for each vibrational level, we have plotted the average angular momentum for each vibrational product. The widths of the angular momentum distributions are indicated by the error bars. In both the $O(^1D)$ + methane and the $O(^3P)$ + HCl reactions, the angular momentum distributions are shifted to lower values of N or j when the reactant is incorporated into a complex.

This decrease in the angular momentum that is expressed in the OH products is a result of the fact that the M•OH vdW complex is longer lived than the collision complex. This difference in lifetimes is not surprising in the case of the $O(^3P)$ + HCl reaction because it proceeds over a barrier. Since it is energetically downhill to go from the transition state to the products, much more kinetic energy is transferred to the departing chlorine atom than to the other atoms or molecules in the cluster. Consequently, the weakly bound complex lives significantly longer than the collision complex and there is time for rotation to translation energy transfer to occur.

For the above argument to apply to the $O(^1D) + (CH_4)_n$ reaction, it must also proceed over a barrier, at least in the case when OH products with low angular momentum are formed. This is contrary to what we would expect from the monomeric

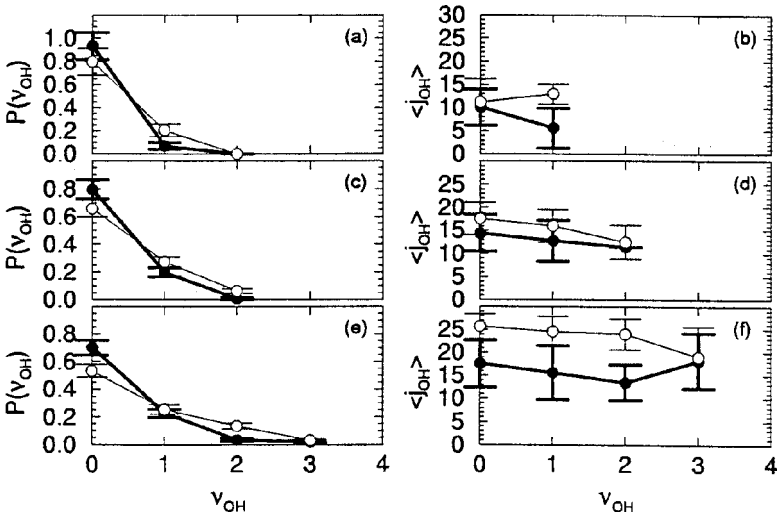

Figure 6. Product state distributions for the OH products formed from the O(^{3}P) + HCl (○) and Ar•HCl (●) reactions at (*a*), (*b*), (*c*), (*d*) 2 eV and (*e*), (*f*) 3.28 eV collision energies. The left-hand column provides vibrational energy distributions while the average angular momentum is plotted in the right-hand column. The error bars for the vibrational energies represent one standard deviation, while those for the average angular momentum provide a measure of the width of the angular momentum distributions, as described in the text. (Reprinted, with permission, from [31].)

case where it is known that the reaction proceeds by an insertion mechanism. To understand the mechanism for the observed rotational cooling in reactions of O(^{1}D) with methane clusters, we return to a discussion of figure 3(*b*). At this geometry, there is a crossing between the O(^{3}P) and O(^{1}D) + HR surfaces which is spin forbidden for the monomeric process but which can be accessed when methane is incorporated into a cluster. The crossing becomes more favourable for reactions of clusters because the introduction of additional methane molecules breaks the total symmetry of the system. It also increases the collision complex lifetime, thereby providing the system more time to access this second mechanism. If the system undergoes the crossing from the singlet to the triplet surface in the reactant channel, then the reaction will occur by means of an abstraction mechanism. This mechanism favours collinear O–H–R collisions and will result in lower angular momentum being expressed in the products. In addition, by conservation of electronic angular momentum, this mechanism also favours the formation of OH in the $^2\Pi_{3/2}$ spin–orbit state over the $^2\Pi_{1/2}$ state, as is reflected in the distributions, plotted in figure 7(*b*).

If, on the other hand, the system reacts on the O(^{1}D) surface, the products will be generated with higher angular momentum and no preference for either of the two spin–orbit states of the OH product should be observed. In fact, comparing the high-energy end of the angular momentum distributions from the reaction of methane and clusters of methane, little difference is observed. Both distributions appear to peak at around $N = 12$ and extend beyond $N = 13$. Similar behaviour can be seen in the results of classical studies of the O(^{1}D) + HCl reaction, plotted in figure 8. As in the reaction of O(^{1}D) with hydrocarbon molecules, this reaction is exothermic and proceeds by forming a long-lived intermediate HOCl complex. As can be seen in the results plotted here, there is little difference between the angular momentum distributions arising

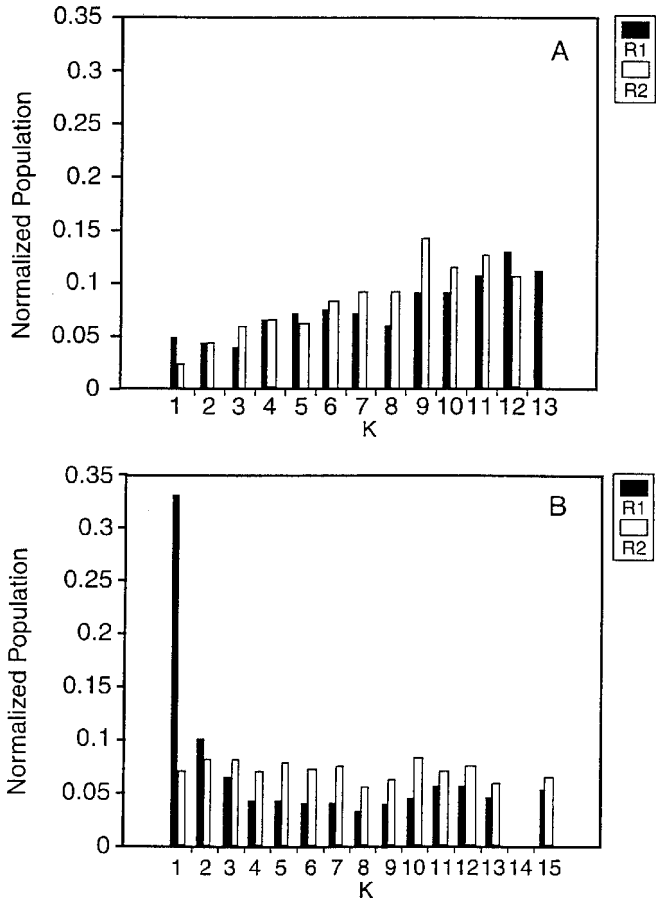

Figure 7. The rotational state distribution of OH ($v = 0$) from the reactions of $O(^1D)$ with (*a*) CH_4 and (*b*) CH_4 clusters. The populations in the electronic sublevels $^2\Pi_{3/2}$ (black bars) and $^2\Pi_{1/2}$ (white bars) are normalized. (Reprinted, with permission from [29].)

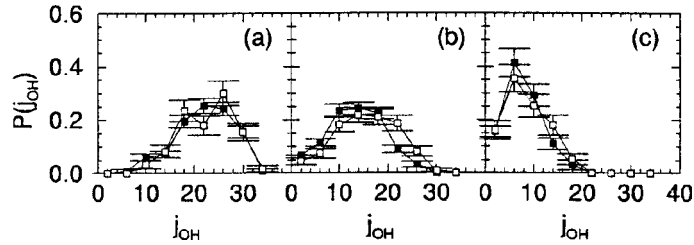

Figure 8. Angular momentum distributions of the OH products that correspond to (*a*) $v = 1$, (*b*) $v = 3$ and (*c*) $v = 5$, formed from the reactions of $O(^1D)$ with HCl (□) and Ar•HCl (■). (Reprinted, with permission, from [31].)

from the reaction with HCl and Ar•HCl. Unlike the reactions on the triplet surface, the reactions on the singlet surface proceed through the formation of a long-lived collision complex, which is lower in energy by several electron volts than either the reactants or products. Consequently, there is sufficient excess energy to eject the other molecules in the complex during the collision complex lifetime. This will cause less energy to be

available to be expressed in the vibrational degree of freedom of the OH product but will have only a small effect on the overall angular momentum distribution of the OH products. In the discussion that follows, we shall investigate these and other systems in more detail, looking for the various effects of complex formation on the dynamics and products of a variety of reactions of atomic oxygen.

5. Specific reactions

5.1. *Association reactions of* $O(^3P)$

To start, we shall consider the effect of complex formation on association reactions [19, 20]. This type of reaction is unique, since the reactions cannot occur without a third 'body' that will take energy and stabilize the reaction product. Namely the pure 'monomeric' process does not occur, unless energy can be taken by a photon. Therefore, the ability to form complexes allows us to investigate association processes that occur in condensed phase but could not be investigated in the past in a controlled manner, as can be done in a crossed-molecular-beam set-up. Specifically we shall focus on the reactions

$$CO \cdot R_m + O(^3P) \rightarrow CO_2^* + mR,$$
$$NO \cdot R_m + O(^3P) \rightarrow NO_2^* + mR.$$

In these reactions, R_m represents spectator atoms or molecules and CO_2^* and NO_2^* represent electronically excited states of the product.

In the case of the reaction of CO, we found that, when an expansion of neat CO was used, the reaction efficiency increased nearly linearly with increasing CO pressure. When CO is expanded with argon, neon or helium, a stronger pressure dependence on the cross-section is observed than for the neat CO expansion. This is an indication of a larger m dependence for these expansion conditions. When the pressure is further increased, the cross-section decreases, indicating that there is some cluster size beyond which the reaction no longer occurs. In general, the cross-sections for the mixed expansions are smaller than for the neat expansion, for the same total pressure. These effects can be clearly seen in the results plotted in figure 9. Increasing the Ar:CO ratio in the mixture from 19.3:1 to 77:1 increases the intensity slightly, whereas increasing the He:CO ratio decreases the intensity, as is demonstrated by the results in table 1.

These results provide information on the effect introducing of one or more spectator atoms or molecules to $O(^3P)$ + CO association reaction. In particular, they show that, when the *spectators* are in a vdW complex with CO, they can substitute for the third body in the corresponding collision process. Small clusters of neat CO, that are probably dimers [19], are found to be more reactive than complexes in which one or two rare-gas atoms are attached to the CO molecule, as is indicated by the lower intensity arising from the Ar/CO or He/CO expansions than for the neat CO expansion at lower pressures. Two competing effects lead to the above observations. First, as the cluster size increases, more vibrational degrees of freedom are available to accept the excess energy from the $CO \cdot O \cdot R_m$ collision complex. This will promote the formation of a stable CO_2^*. This effect is responsible for the increase in the intensity with increasing pressure observed under all three of the experimental conditions, plotted in figure 9. In addition, as the number of helium or argon atoms in the complex increases, they can effectively screen the reactive site, thereby leading to the observed decrease in intensity at the highest pressures that we investigated. When there are one to four helium or argon atoms, this screening is only partial, but for $CO \cdot R_m$ complexes with $m > 4$, the screening is nearly complete and the reactivity falls off with increasing

Table 1. Comparison of the theoretical and experimental ratios for a variety of CO–rare-gas mixture compositions. The experimental ratio represents the ratio of pressures necessary to yield a given signal intensity and the masses used to compute the theoretical ratio is given by $(m_1/m_2)^{1/2}$, where m_i represents the weighted average of the masses of the species in the mixture.

Mixtures	CO: rare gas	R_{expt}	R_{theory}
$\frac{CO/He}{CO/Ar}$	1:77	3.6	3.04
$\frac{CO/He}{CO/Ar}$	1:19.3	2.0	2.76
CO/He	1:77 to 1:19.3	1.8	1.09
CO/He	1:38.6 to 1:19.3	1.2	1.06
CO/Ar	1:77 to 1:19.3	0.9	1.00

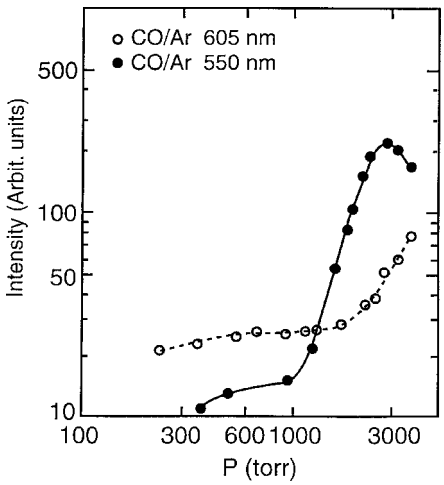

Figure 9. The signal dependence on the pressure for constant-composition beams of CO, CO–He and CO–Ar. (Reprinted, with permission, from [19].)

m. The above effects are primarily steric and energetic. We shall see that a similar combination of effects can also be seen in bimolecular reactions when we compare the cross-sections for reactions of $O(^1D)$ and $O(^3P)$ with HCl and Ar•HCl.

To understand the dependence of the chemilumenescence intensity on the CO: Ar or CO: He ratio, we need to consider the role of the average mass of the expansion on the size of clusters. In particular, to obtain a similar cluster distributions for two different expansion conditions, Hagena [32] has argued that the pressures should be related by

$$P_2 = P_1 \left(\frac{m_1}{m_2}\right)^{1/2} \tag{1}$$

where m_i provides the average mass of the expansion mixture. A comparison of the observed and predicted pressure dependences is given in table 1. Overall, the agreement is quite good, which argues that the observed differences between the different mixed expansions can be rationalized solely on the grounds of different cluster size distributions for a given pressure. Therefore, the most important factor in determining

the cross-section is the cluster size and overall CO/rare-gas composition and not the details of which rare-gas atom is present.

If we turn our attention to the reaction of NO with $O(^3P)$, the situation is somewhat different. First, we find that the chemilumenescence intensity increases as the third power of the pressure. This result is independent of the composition of the expansion—neat NO, NO/Ar or NO/He. Further, analysis of the angular distributions indicate that because NO dimers are particularly stable species. In contrast with CO where $(CO)_2$ and Ar•CO are both expected to be bound by 50–100 cm^{-1} [33, 34], the NO dimer [34] has binding energies of approximately 550 cm^{-1} compared with Ar•NO [35], which is bound by approximately 100 cm^{-1}. Therefore, whereas the results for CO come from a variety of complexes of CO with the rare-gas atoms in the beam, the observed signal in the NO experiments arose primarily from $(NO)_2$.

The fact that the cross-section increases as the third power of the pressure, rather than as the square, indicates that this is a non-equilibrium process. Instead, the pressure dependence of the cross-section should be formulated in terms of kinetic equations from which a cubic dependence is obtained. This dependence is expected when, as in this case, the dissociation energy of the cluster is larger than the collision energies. This situation is in contrast with the observations for the CO system where the expansions were in equilibrium.

5.2. *Exchange reactions of $O(^3P)$ with saturated hydrocarbons*

The reaction of $O(^3P)$ with small saturated hydrocarbon molecules is known to proceed via a collinear abstraction mechanism, in the gas phase [36]. This process results in the production of rotationally cold OH products. However, in reactions of $O(^3P)$ with large saturated hydrocarbon molecules, the OH rotational distribution becomes statistical [37]. Moreover, in reactions in solution or in neat liquids, the alcohol, rather than OH, is the primary product. Two possible explanations for this result are firstly recombination of the R + OH reaction products or secondly the reaction crossing from the $O(^3P)$ to the $O(^1D)$ reactive surface on which the reaction proceeds through an insertion mechanism. The first of these possibilities has been ruled out by the fact that in reactions of chiral hydrocarbon the initial configuration was retained [38].

When the reaction of $O(^3P)$ with cyclohexane was studied in a crossed-molecular-beam set-up [24], it was found that cyclohexanol is formed when clusters are present in the beam. It has been suggested that, in the reactions with cyclohexane clusters, the collision complex lifetime is increased, compared with that for the monomeric process [16]. This will enhance the intersystem crossing between the triplet and the underlying singlet surface [39]. As is the case for reactions of $O(^1D)$ with saturated hydrocarbons, the $O(^1D)$ with cyclohexane reaction occurs through an insertion mechanism. This mechanism may also be responsible for the formation of alcohols when $O(^3P)$ reacts with large hydrocarbons and in the liquid phase. In addition, this mechanism explains the more statistical rotational distribution of the OH that is formed from reactions of large saturated organic molecules compared to that resulting from reactions of methane. As we discussed in section 2.1, the idea that even a single atom, when attached to the hydrocarbon, can increase significantly the collision complex lifetime is supported by classical simulations and this increase in the complex lifetime will facilitate the necessary curve crossing for this reaction [16].

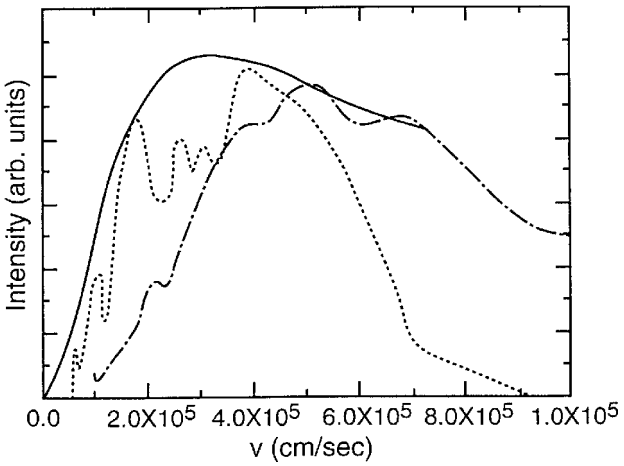

Figure 10. Velocity distributions of the OH ($v = 0$; $N = 1$) from reactions of O(^{1}D) with propane (——), methane (—·—) and methane clusters (-----). The velocities are obtained in the centre-of-mass frame and in the methane clusters; the remaining cluster fragment is assumed to have infinite mass. (Reprinted, with permission, from [29].)

5.3. *Exchange reactions of O(^{1}D) with saturated hydrocarbons*

We have already alluded to some of the features of the reactions of O(^{1}D) with hydrocarbon clusters in section 4. In the discussion that follows, we shall focus on some of the features that are unique to these systems. We shall focus on the effects of complex formation on the rotational, vibrational, electronic and Λ-doubling state population distributions and translational energy distributions of the OH in $v = 0, 1$ emerging from the reactions of O(^{1}D) with methane and propane.

As was described above, significant vibrational and rotational cooling are observed in the OH products when methane clusters are reacted, compared with the product state distributions resulting from reactions of the monomers. In addition, we find that the kinetic energy of the OH that is formed from the reaction of methane clusters is lower than that resulting from the monomeric process. This is illustrated by the OH velocity distributions, plotted in figure 10. In the case of the monomeric reaction, the OH emerges with a very broad velocity distribution peaking at 5×10^5 cm s^{-1}. When methane clusters are allowed to react, the OH velocity distribution is narrower and has two peaks at 1.5×10^5 and 3.6×10^5 cm s^{-1}. These peaks probably arise from the two mechanisms for the reaction of methane clusters with O(^{3}P), with the fast OH resulting from the abstraction process occurring on the triplet surface, while the slower OH emerges from the insertion reaction that takes place on the singlet potential energy surface.

The observed vibrational and translational cooling of the products of the reactions of O(^{1}D) with methane clusters, compared with the monomeric process, are due to kinematic factors. The similarity of the masses of the complexing methane molecules and the approaching oxygen atom imply that momentum will be transferred very efficiently to this 'third body'. In addition, the departing methane molecule may take away a fraction of the exothermic as kinetic energy. This will manifest itself in the colder translational energy distributions, plotted in figure 10, as well as the cooler vibrational energy distributions of the OH products, described above.

This loss of energy to the clustering molecules also implies that the dissociation process will be slower when clusters are involved compared with the monomeric

reaction. While dissociating, the collision complex undergoes out of plane rotations. Because of the increase in the ratio between the collision complex lifetime and rotational period of OH, the two Λ-doubling components of the OH products mix, and the preference for the A´ state that has been observed for the monomeric process [29] vanishes. Experimentally, we observe that the population ratio between the two Λ-doubling components follows the unconstrained dynamics model, implying that the OH is free to rotate during the dissociation of the complex. These effects have been attributed to contributions from the abstraction mechanism [40], or to a long-lived collision complex that dissociates after the energy has been equilibrated [41].

When the same changes in the experimental conditions are made for the propane system, some rotational cooling is observed, but the effect is much smaller. In addition, the reactions of $O(^1D)$ with propane monomers result in OH products that are rotationally colder than the products that resulted from reactions of $O(^1D)$ with isolated methane molecules. In both cases, we find that there is a high probability for forming OH in its $^2\Pi_{3/2}$ spin–orbit state with $N = 1$.

These features are interconnected and provide a database for a comprehensive understanding of the reaction dynamics of $O(^1D)$ reactions with clusters of methane. Methane, in contrast with all larger saturated hydrocarbons, is a rather rigid molecule, containing only high-frequency vibrational modes. Methane clusters, on the other hand, have low-frequency modes that are associated with the vdW interactions. In this way, methane clusters resemble a large hydrocarbon molecule and the reaction of these species can be explained by analogy with the dynamics of such systems. The existence of low-frequency modes in the cluster and in larger hydrocarbon molecules leads to stabilization of the collision complex and lengthening of its lifetime. As is verified by classical trajectory simulations, the longer complex lifetime allows the oxygen to sample larger regions of the phase space. Consequently, the probability for curve crossing from the singlet to the triplet potential energy surface is enhanced. If the electronic angular momentum is conserved in this transition, oxygen in its $^3P_2$ state will be formed. Since the reactants are rotationally cold and the angular momentum associated with the transferred hydrogen atom is small, the electronic angular momentum provides the main contribution to the total angular momentum and therefore is conserved in the process. By following the electronic correlation curves, the OH product should emerge with a preference for the $^2\Pi_{3/2}$ electronic state [30].

We believe that the reaction mechanism, in which curve crossing takes place during the lifetime of the collision complex, is a general mechanism in the reactions of oxygen atoms as we have also seen it in reactions of $O(^3P)$ with cyclohexane dimers, described in the next section. These phenomena shed new light on the effect of solvent molecules on the reaction dynamics. By introducing low-frequency modes into the system, the solvent molecules stabilize the collision complex, allowing the system to explore more areas of phase space for longer time, and non-adiabatic transitions to become more probable [39].

5.4. *Reactions of $O(^1D)$ and $O(^3P)$ with HCl complexes*

Unlike the reactions of atomic oxygen with hydrocarbons, described above, our studies of the reactions of oxygen with HCl, $(HCl)_2$ and Ar•HCl have been performed under conditions such that these reactions are occurring on a single potential surface. As such, we shall consider the reactions of $O(^3P)$ and $O(^1D)$ as separate processes.

Before considering the effects of complexation on the dynamics of these reactions, it may be helpful to consider the differences in the energetics of the two reactions,

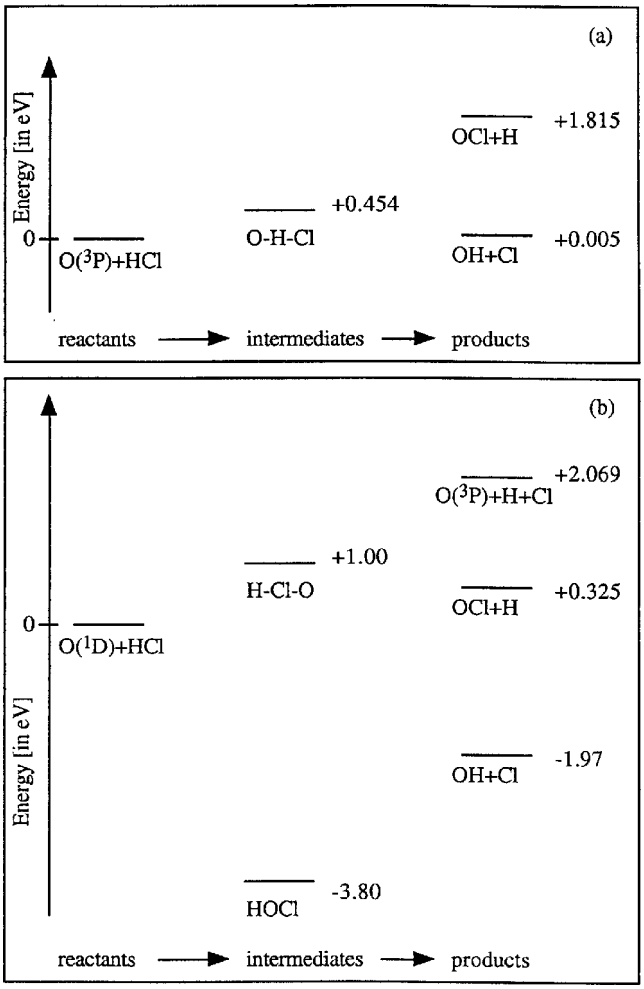

Figure 11. The energetics of the reactions of (*a*) $O(^3P)$ and (*b*) $O(^1D)$ with HCl. the reported energies are based on the Koizumi *et al.* [42] and Schinke[43] potentials respectively. All energies are reported in electron volts, with the reactant's energy defining the zero in energy. (Reprinted, with permission, from [31].)

shown in figure 11. These plots are based on the $O(^3P)$ + HCl potential of Koizumi *et al.* [42] and the $O(^1D)$ + HCl potential of Schincke [43]. According to these potentials, the $O(^1D)$ + HCl reaction that forms OH is exothermic by 2 eV, with a strongly bound HOCl intermediate, while the reaction that forms OCl is endothermic by 0.3 eV and may proceed either by going through the formation of the HOCl complex or by forming a H–Cl–O collision complex, which is 1 eV higher in energy than the reactants. Finally, the reaction of $O(^3P)$ with HCl to form OH is thermoneutral and has a barrier of approximately 0.45 eV.

In the case of the reaction of $O(^3P)$ with HCl at low to moderate collision energies, electronic effects appear to dominate. For example, at collision energies of, on average, 0.136 eV, time-dependent calculations of the reaction probabilities on two *ab initio* based potential surfaces [42, 44] predict reaction probabilities in the range of 10^{-6}–10^{-5} [45]. When the HCl is incorporated into $(HCl)_2$, the reaction probability

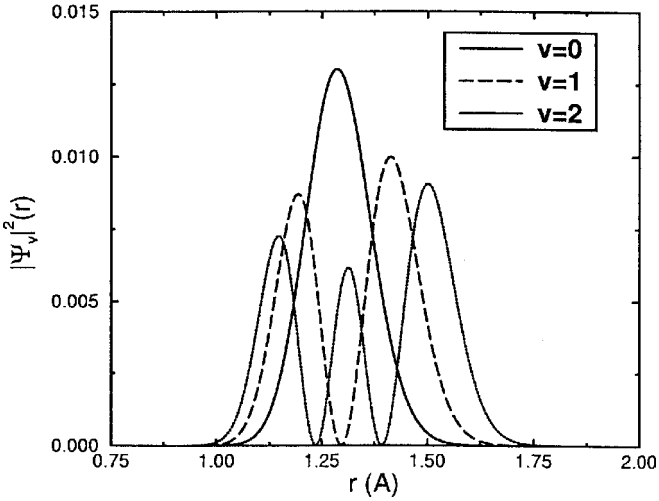

Figure 12. The probability density associated with the three lowest-energy states of HCl.

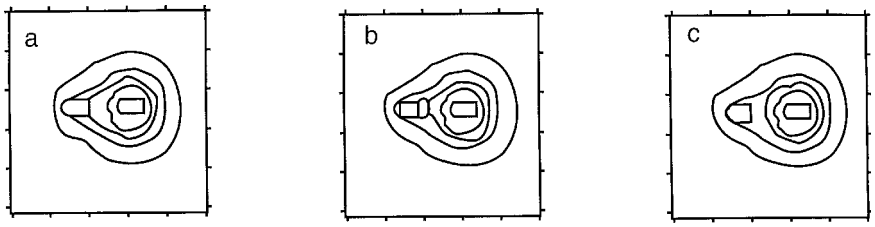

Figure 13. The electron density contour map (*a*) for HCl in its ground state, $r = 1.247$ Å, and (*b*), (*c*) for HCl with bond lengths of (*b*) 1.35 Å and (*c*) 1.45 Å, corresponding to excitation to $v = 1$ and $v = 2$ respectively. The contour lines are drawn and represent -0.001, -0.005, -0.01, -0.02 and 0 from the outside inwards. (Reprinted, with permission, from [46].)

increases by approximately three orders of magnitude to 10^{-3} [46]. If we compare this result with the changes to the reaction probability brought about by excitation of the HCl bond into $v = 1$, we find that vibrational excitation leads to an increase in the rate constant by two orders of magnitude [47, 48]. According to quantum calculations [45, 49] on the Koizumi *et al.* potential, excitation of HCl to $v = 1$ leads to a factor of 1000 increase in the reaction probability. The mechanism, for the observed increase in reactivity with excitation of the HCl vibration, is well understood. By exciting the HCl stretch, one is effectively putting energy into the reaction coordinate. Consequently, the reaction probabilities, obtained when HCl is in its first excited state, are typically much larger than those obtained when the energy is put into other degrees of freedom, for example translation or rotation [45, 49].

From an electronic standpoint, the increase in reactivity from HCl ($v = 1$) can be seen as a reflection of the increase in the probability amplitude at larger values of r, shown in figure 12. While the most probable HCl distance is 1.29 Å when $v = 0$, at $v = 1$ or 2, this distance is increased to 1.58 and 1.65 Å, respectively. As the HCl bond is allowed to extend, the electron density on the hydrogen is reduced. This is illustrated in electron density plots shown in figure 13, where the electron densities are plotted when the HCl distance is 1.25, 1.35 and 1.45 Å. These densities are calculated within

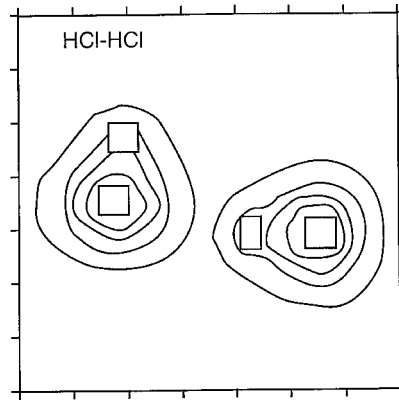

Figure 14. The electron density contour map for HCl dimer in its equilibrium configuration. A cut through the ClHCl plane is presented. The values for the contour lines are the same as those used in figure 13. (Reprinted, with permission, from [46].)

the generalized valence bond treatment with restricted configuration interaction for the monomer and second-order Möller–Plesset perturbation theory is used in the calculations on $(HCl)_2$. In both cases, a 6-31G** basis set is used.

If we compare the above results to the electron density distributions for the HCl monomers in $(HCl)_2$, plotted in figure 14, we find a similar decrease in the electron density in the HCl monomers upon complexation. This decrease in the electron density on the hydrogen atoms can be viewed as a result of charge transfer from the proton to the chlorine atom when the vdW bond is formed.

One way to rationalize the barrier to the $O(^3P) + HCl$ reaction is in terms of the hydrogen atom in HCl being embedded inside the electronic density of the chlorine atom, as is shown in figure 13(*a*). In order for reaction to occur when HCl is in this configuration, the oxygen atom will need to penetrate the repulsive electron cloud before it can react. Within this picture, enhancement of reactivity upon vibrational excitation of HCl can be seen to result from the hydrogen atom moving further away from the electron density around the chlorine atom. This effectively thins the repulsive electron cloud that the oxygen atom must penetrate in order to react. The larger the amplitude of the HCl vibration, the thinner is the effective electron cloud. Similar thinning of the electron clouds around the hydrogen atoms is oberved in $(HCl)_2$. In this case, the weakening comes from the transfer of electron density away from the so-called hydrogen bonding proton towards the chlorine end of the other monomer. This charge transfer effectively reduces the electron density around this hydrogen, making it potentially more reactive than the free HCl molecule. This effect is expected to be comparable with that obtained from vibrational excitation.

In addition to changes in the electron density, we should also consider kinematic effects of complex formation on the reaction cross-section [31]. To investigate these effects we have used classical trajectory simulations. Because the simulations are purely classical, tunnelling is not included in the calculations and we are forced to consider much higher collision energies, those in the range of 1–3 eV. For these simulations, we use the potential of Koizumi *et al.* [42] to describe the interactions between $O(^3P)$ and HCl. The potential of Schinke [43] is used to describe the $O(^1D) + HCl$ reaction. The intermolecular interactions are included through the introduction of an argon atom through pairwise additive Ar•O, Ar•H and Ar•Cl

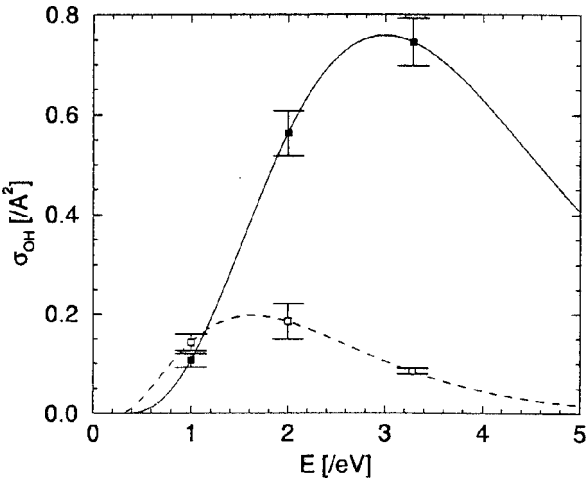

Figure 15. The cross-section for OH formation for the reactions of O(^{3}P) with HCl (□) and Ar•HCl (■). The cross-sections have been fitted to excitation functions, described in the text. The error bars for each result represent one standard deviation. (Reprinted, with permission, from [31].)

potentials [46]. Although these energies do not correspond directly to the experimental conditions, studies of the classical cross-sections at these energies provide insights into possible kinematic effects on the reactivity of systems incorporated into vdW complexes. In figure 15 the cross-sections for the reactions of O(^{3}P) with HCl and Ar•HCl are plotted as functions of the collision energy. This reaction is approximately thermoneutral with a barrier of 0.45 eV, and it is classically forbidden for collision energies below 0.45 eV. As such, the excitation function is expected to take the form [50]

$$\sigma_E = C(E - E_{th})^n \exp[-m(E - E_{th})]. \quad (2)$$

We take E_{th} to be the difference between the barrier height and the zero-point energy of the HCl, and C, m and n are chosen to reproduce the three calculated values of $\sigma_{OH}(E)$. Clearly with as many parameters as data points, we have no way to check the reliability of the parameters, but we use the resulting curves to investigate general features of the effects of complexation on the O(^{3}P) + HCl reaction.

To understand the observed trends, we need to consider three effects of the introduction of an argon atom to the system. First, the introduction of the argon atom increases the effective size of the complex. This can be seen by comparing the minimum Ar•HCl distance of 4.00 Å [51] with the HCl bond length, which is only 1.27 Å [52]. Because of these differences, the effective size of Ar•HCl is more than twice that of HCl. This increase in size should increase the cross-section. One must also consider the fact that the argon atom will remove a fraction of the collision energy from the collision complex. For the O(^{3}P) + HCl reaction, we find that, on average, the argon atom leaves with 10% of the initial relative translational energy. This will lower the energy available for the O + HCl reaction and will effectively shift the curve given by equation (2). Finally, the argon atom can block the formation of the collision complex. This effect can be understood in terms of the fact that the minimum-energy configuration of Ar•HCl corresponds to the argon, hydrogen and chlorine atoms

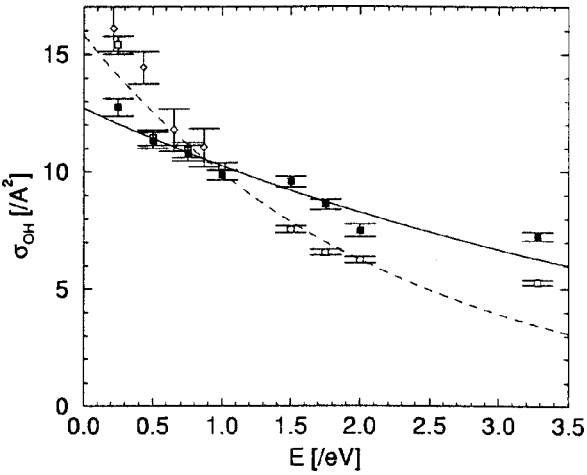

Figure 16. The cross-sections for OH formation for the reactions of O(^{1}D) with HCl (□) and Ar•HCl (■). The cross-sections for the O(^{1}D) + HCl reaction reported in [43] are also shown (◇). The calculated cross-sections have been fitted to excitation functions, described in the text. Error bars for each result represent one standard deviation. (Reprinted, with permission, from [31].)

being collinear, with the hydrogen atom between the other two. On the other hand, the O–H–Cl transition state occurs when the O–H–Cl angle is approximately 133°. When the zero-point energy in the Ar•HCl bend is considered, the argon atom may completely block the formation of an O–H–Cl transition state complex, thereby decreasing the cross-section for the reaction.

At low collision energies $\sigma_{OH}^{(HCl)} > \sigma_{OH}^{(Ar\bullet HCl)}$, and steric effects appear to dominate. At higher energies, the cross-section for OH formation is as much as four times larger for collisions with Ar–HCl than for collisions with HCl. We conclude that at higher collision energies the increase in the size of the HCl complex is an important factor in the increase in the cross-section. Finally, the shift in the peak in the excitation function can be attributed to the loss of, on average, 10% of the collision energy to translation of the argon atom.

The reactions of HCl and Ar•HCl with oxygen in its first excited electronic state display similar effects. Because this reaction is endothermic and proceeds through the formation of a strongly bound OHCl intermediate, we expect that the cross-sections will decay approximately exponentially with collision energy [50]. The calculated cross-sections for eight collision energies between 0.25 and 3.5 eV are plotted as open squares in figure 16. We fit these points to the excitation function

$$\sigma_E = C\exp(-mE) \tag{3}$$

with $C = 15.81$ Å^2 and $m = 0.465$ eV^{-1}. The function also reproduces the cross-sections reported by Schinke [43], plotted as open diamonds in this figure. The cross-sections for OH formation from reactions of O(^{1}D) with Ar•HCl are plotted as full squares. These were also fitted to the excitation function in equation (3). Here $C =$ 12.70 Å^2 and $m = 0.214$ eV^{-1}.

An interesting feature of the cross-sections for these reactions is that, while at lower collision energies the cross-section $\sigma_{OH}^{(Ar\bullet HCl)}$ for the reaction with Ar•HCl is

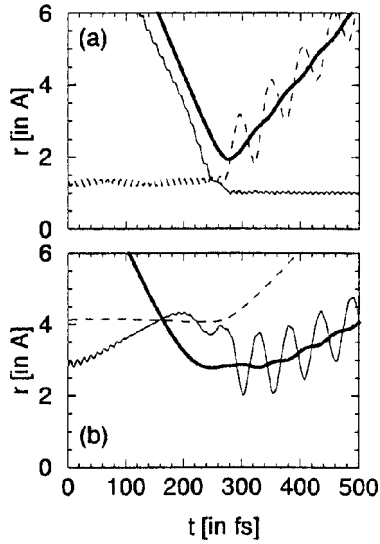

Figure 17. A representative $O(^3P) + HCl$ trajectory: (*a*) the OH (——), OCl (——) and HCl (– – –) distances plotted as functions of time; (*b*) the ArO (——), ArCl (– – –), and ArH (——) distances plotted as functions of time.

smaller than the cross-section $\sigma_{OH}^{(HCl)}$ for reactions of HCl, at higher energies, $\sigma_{OH}^{(Ar\bullet HCl)} > \sigma_{OH}^{(HCl)}$. To understand the observed trends, we need to consider three effects of the argon atom on the system, as described above.

Given the observed relative trends in $\sigma_{OH}^{(HCl)}$ and $\sigma_{OH}^{(Ar\bullet HCl)}$, we believe that the steric effects represent the dominant effect of the introduction of an argon atom when the collision energy is low. At the highest collision energies, we find that

$$\sigma_{OH}^{(HCl)}(E) \approx \sigma_{OH}^{(Ar\bullet HCl)}(E - \langle E_{Ar} \rangle), \tag{4}$$

where $\langle E_{ar} \rangle$ represents the average kinetic energy of the argon atom for these collisions. This leads us to conclude that the energy effect of the argon atom is more important than the size effect for this particular reaction. Similar behaviour has been observed by Varandas and co-workers [53] in their studies of reactions of H with $Ar\bullet O_2$.

Another effect that needs to be considered in the discussion of the effects of complexation on the reactions of $O(^3P)$ and $O(^1D)$ with HCl comes in the relative lifetimes of the collision complexes in the presence and absence of a complexing agent. In particular, we are interested in how differences in lifetimes, brought about by introducing a third body, will affect the product state distributions for the reaction of interest. Based on the results described above for reactions with hydrocarbon clusters, we know that an important effect of complexation is in cooling the reaction products. The mechanism of this is clearly illustrated in the trajectory that was obtained for the $O(^3P) + Ar\bullet HCl$ reaction, shown in figure 17. Because the argon atom departs from the collision complex with, on average, less kinetic energy than the chlorine atom, the effective lifetime of the Ar•OH vdW complex is longer than that of the collision complex. This longer-lived Ar•OH vdW complex will result in the observed rotational cooling of the OH product. In contrast, because the $O(^1D) + HCl$ proceeds through a long-lived, strongly bound HOCl collision complex, some of the excess energy will be used to eject the argon atom. As a result, in this reaction, the collision complex lives,

on average, longer than the vdW complex and as a result much less rotational cooling has been observed in this reaction than in the $O(^3P) + HCl$ reaction [54].

5.5. *Reactions of $O(^1D)$ with water clusters*

As was alluded to in section 3 above, reactions of $O(^1D)$ with water clusters provide a distinct situation from the reactions with HCl or saturated hydrocarbons. This difference is a reflection of the unusually strong intermolecular forces that hold water clusters together. In the case of small clusters, dimers and possibly trimers, we find that less internal energy is expressed in the OH product than was the case for the monomeric process. In the case of medium-sized clusters, with up to seven or eight water molecules, a statistical distribution of internal energy is observed, while large clusters do not produce any OH product.

While many features of the dynamics of this reaction are similar to those of the reactions, described above, there are some notable differences. First, in contrast with the other reactions described above, the reaction of $O(^1D)$ with water produces two OH products. The new OH is formed by the hydrogen atom that was removed from the water molecule and takes the same role as the OH product of the other reactions. The old OH is the *spectator* OH molecule that remains after H_2O has lost a hydrogen atom. This OH takes on the role of Cl in the $O(^3P) + HCl$ reaction or R in the reactions with hydrocarbons. When we detect the OH that is formed by reactions of $O(^1D)$ with water clusters, we cannot distinguish between the new and the old OH molecules. In addition, unlike the reactions of $O(^1D)$ with hydrocarbon molecules, there appear to be multiple size regimes over which the OH product state distribution evolves. Based on the dependence of the OH vibrational state distribution on the collision energy, we believe that the $O(^1D) + H_2O$ reaction is proceeding through an abstraction mechanism, analogous to that observed in the $O(^3P) + HCl$ or HR reactions [55]. Finally, for small water clusters, we observe different rotational distributions for the two spin–orbit states for all values of N, and not just for low N, as was shown in figure 7.

In the case of water dimers, the kinematics of the reaction are similar to those of the $O(^3P) + Ar{\bullet}HCl$ reaction, described above. In this case, the old OH products take on the role of the chlorine atom and will escape the complex rapidly. Therefore, we do not expect that this OH product will undergo significant rotational cooling. On the other hand, the new OH is expected to remain in the complex for some time before the $OH{-}H_2O$ complex is fully dissociated. This will lead to rotational cooling of the new OH product when it is formed from reaction with the water dimer compared with reactions with the water monomer. This cooling is somewhat masked in figure 5(*a*) by the fact that both monomers and dimers are present in the beam. Another feature of the OH product state distributions that differs from that observed for the reactions with hydrocarbon clusters, is the nearly monotonic decrease in the population in the $^2\Pi_{3/2}$ with increasing N. In the case of the reactions with hydrocarbon clusters, this distribution was clearly bimodal with a second peak at large N.

When larger clusters of water are allowed to react, the angular momentum distributions for the $^2\Pi_{3/2}$ and $^2\Pi_{1/2}$ spin–orbit states are similar. This result reflects the fact that the larger binding energy of water clusters, compared with the hydrocarbon clusters, makes it more difficult for the cluster to dissociate following reaction. Further, the structure of the water clusters makes it likely that the old OH will become trapped in the cluster. Since both of the OH products are associated with a massive partner, they will be thermalized during the complex lifetime. As the clusters become larger, with more than seven or eight water monomers, the lifetime of the water cluster,

after the reaction, is sufficiently long for the two OH products to have time to recombine. Consequently, we are unable to observe OH products reactions of $O(^1D)$ with clusters with more than approximately eight water molecules.

6. Summary and conclusions

The chemistry of oxygen atoms and how it is affected by the introduction of solvating atoms or molecules is of importance if we are to understand many important processes in nature, from atmospheric chemistry to biochemistry. Beyond its practical relevance, the fact that oxygen atoms have a very low first excited electronic state makes their reactivity a sensitive tool for investigating the variation in reaction mechanisms induced by the solvent. Despite the experimental difficulties in studying neutral clusters, the information obtained so far allows us to derive several conclusions on the effects of the 'solvent' molecules on chemical reactions. Specifically, reactions in clusters lead to the following.

(1) The collision complex lifetime is lengthened, which may result in efficient surface crossing.
(2) There exist internal energy distributions in the products that depend on the difference between the collision complex lifetime and the lifetime of the vdW complex. If the vdW complex dissociates before the reaction ends, the introduction of a third body has little effect on the rotational energy distribution. However, in most cases, the vdW bonds survive beyond the collision complex lifetime and therefore the products emerge with less internal energy than in the monomeric process.

In addition, we find that the complex size effect depends on two parameters: the size of the molecules from which the complex is formed and the coupling between the units in the complex. When the monomer is already a 'large molecule', namely it contains many internal degrees of freedom, then the cluster formation has almost no effect on the reaction. However, the formation of complexes from 'small molecules' has a large effect on the reactivity. If the constituents of the complex are weakly coupled, then the exact size of the complex is of essentially irrelevant. However, for strongly bound complexes (such as water clusters), the exact size will affect the reaction mechanism and the products formed.

Experimental difficulties in performing size-selective studies on the reactions of vdW molecules and the multidimensionality of the problem are probably the reason why relatively few studies on the subject have been performed either experimentally or theoretically. Advances in both directions are required in order to gain further insights into this field. These will be of great importance if we are to understand the relationship between how reactions occur in the gas phase and processes that take place in a more 'realistic' chemical environment, namely the condensed phase.

Acknowledgements

We would like to acknowledge the support of the US–Israel Binational Science Foundation and our students and post-doctoral researchers whose hard work led to many of the findings described in this review. In addition, A.B.M. acknowledges support from the (US) National Science Foundation under grant CHE-9732998 through the CAREER program, the Ohio State University Board of Regents and the donors to the Petroleum Research Fund, administered by the American Chemical Society.

References

[1] (a) Dixon, D. A., King, D. L., and Herschbach, D. R., 1975, *J. Am. chem. Soc.*, **97**, 6268; (b) Worsnop, D. R., Buelow, S. J., and Herschbach, D. R., 1981, *J. phys. Chem.*, **85**, 3024.
[2] Elliot, E. R., 1992, *J. phys. Chem.*, **96**, 10105.
[3] Buck, U., and Ettischer, I., 1998, *J. chem. Phys.*, **108**, 33, and references cited therein.
[4] Gée, C., Gaveau, M. A., Sublemontier, O., Mestdagh, J. M., and Visticot, J.-P., 1997, *J. chem. Phys.*, **107**, 4194.
[5] Hu, X., and Martens, C. C., 1993, *J. chem. Phys.*, **99**, 9532.
[6] Herschbach, D. R., 1976, *Pure appl. Chem.*, **47**, 67.
[7] Naaman, R., 1988, *Adv. chem. Phys.*, **70**, 181.
[8] Breckenridge, W. H., 1989, *Accts chem. Res.*, **22**, 21.
[9] Roncero, O., Halberstadt, N., and Beswick, J. A., 1994, *Reaction Dynamics in Clusters and Condensed Phases*, edited by J. Jortner, R. D. Levine and B. Pullman (Berlin: Kluwer).
[10] Gerber, R. B., McCoy, A. B., and Garcia-Vela, A., 1994, *A. Rev. phys. Chem.*, **45**, 275.
[11] Mark, T. D., and Castleman, A. W., Jr, 1985, *Adv. at. molec. Phys.*, **20**, 65.
[12] Chen, Y., Hoffmann, G., Shin, S. K., Oh, D., Sharpe, S., Zeng, Y. P., Beaudet, R. A., and Wittig, C., 1991, *Adv. molec. Vibrations Collisions*, **1B**, 187.
[13] Bacic, Z., and Miller, R. E., 1996, *J. phys. Chem.*, **100**, 12945.
[14] (a) Frost, G., and Vaida, V., 1995, *J. geophys. Res.-Atmos.*, **100**, 18803; (b) Vaida, V., Frost, G. J., Brown, L. A., Naaman, R., and Hurwitz, Y., 1995, *Ber. Bunsen ges. phys. Chem.*, **99**, 371.
[15] (a) Alagia, M., Balucani, N., Cartechini, L., Casavecchia, P., van-Kleef, E. H., Volpi, G. G., Kuntz, P. J., and Sloan, J. J., 1998, *J. chem. Phys.*, **108**, 6698; (b) Stevens, J. E., Cui, Q., and Morokuma, K., 1998, *J. chem. Phys.*, **108**, 1544; (c) Ramachandru, B., Senekowitsch, J., and Wyatt, R. E., 1997, *Chem. Phys. Lett.*, **270**, 387 (1997); (d) Quandt, R. W., Xuebin, W., Tsakiyama, T., and Bersohn, R., 1997, *Chem. Phys. Lett.*, **276**, 122; (e) Summerfield, D., Costen, M. L., Ritchie, G. A. D., Hancock, G., Hancock, T. W. R., and Orr-Ewing, A. J., 1997, *J. chem. Phys.*, **106**, 1391.
[16] Hurwitz, Y., Rudich, Y., Naaman, R., and Gerber, R. B., 1993, *J. chem. Phys.*, **98**, 2941.
[17] Heller, E. J., 1976, *J. chem. Phys.*, **65**, 1289.
[18] Lufaso, M. W., and McCoy, A. B., 1999 (to be published).
[19] Nieman, J., Schwartz, J., and Naaman, R., 1986, *Z. Phys. D.*, **1**, 231.
[20] Nieman, J., and Naaman, R., 1986, *J. chem. Phys.*, **84**, 3825.
[21] Honma, K., and Kajimoto, O., 1984, *J. chem. Phys.*, **81**, 3344.
[22] Bialkowski, S. E., 1983, *J. chem. Phys.*, **78**, 600.
[23] Cohen, S., and Naaman, R., 1983, *Discuss. Faraday Soc.* **75**, 267.
[24] (a) Rudich, Y., Lifson, S., and Naaman, R., 1991, *J. Am. chem. Soc.*, **113**, 7077; (b) Rudich, Y., Hurwitz, Y., Lifson, S., and Naaman, R., 1993, *J. chem. Phys.*, **98**, 2936.
[25] Ben-Nun, M., and Levine, R. D., 1992, *J. phys. Chem.*, **96**, 1523.
[26] Nieman, J., and Naaman, R., 1984, *Chem. Phys.*, **96**, 407.
[27] Plusquellic, D. V., Votava, O., and Nesbitt, D. J., 1994, *J. chem. Phys.*, **101**, 6356.
[28] Bohac, E. J., and Miller, R. E., 1993, *J. chem. Phys.*, **98**, 2604.
[29] Rudich, Y., Hurwitz, Y., Frost, G. J., Vaida, V., and Naaman, R., 1993, *J. chem. Phys.*, **99**, 4500.
[30] Hurwitz, Y., Rudich, Y., and Naaman, R., 1994, *Israel J. Chem.*, **34**, 59 (1994).
[31] Lufaso, M. W., and McCoy, A. B., 1998, *Chem. Phys.*, **239**, 187.
[32] Hagena, O., 1981, *Surf. Sci.*, **106**, 101.
[33] Jansen, G., 1996, *J. chem. Phys.*, **105**, 89.
[34] Linn, S. H., Ono, Y., and Ng, C. Y., 1981, *J. chem. Phys.*, **74**, 3342.
[35] Schmelz, T., Rosmus, P., and Alexander, M. H., 1994, *J. phys. Chem.*, **98**, 1073.
[36] Andresen, P., and Luntz, A. C., 1980, *J. chem. Phys.*, **72**, 5842, 5851.
[37] Park, C. R., and Wiesenfeld, J. R., 1991, *J. chem. Phys.*, **95**, 8166.
[38] Zadok, E., and Mazor, T., 1982, *Angew. Chem.*, **21**, 303; 1982, *J. org. Chem.*, **47**, 2223.
[39] (a) Tully, J. C., 1993, *J. chem. Phys.*, **61**, 61; (b) Zahr, G. E., Preston, R. K., and Miller, W. H., 1975, *J. chem. Phys.*, **62**, 1127.
[40] Luntz, A. C., 1980, *J. chem. Phys.*, **73**, 1143.
[41] Park, C. R., and Wiesenfeld, J. R., 1991, *J. chem. Phys.*, **95**, 8166.

[42] KOIZUMI, H., SCHATZ, G. C., and GORDON, M. S., 1991, *J. chem. Phys.*, **95**, 6421.
[43] SCHINKE, R., 1988, *J. chem. Phys.*, **80**, 5510.
[44] RAMACHANDRAN, B., SENEKOWITSCH, J., and WYATT, R. E., 1997, *Chem. Phys. Lett.*, **270**, 387.
[45] WANG, L., KALYANARAMAN, C., and MCCOY, A. B., 1999, *J. chem. Phys.* **110**, 11221.
[46] HURWITZ, Y., STERN, P. S., NAAMAN, R., and MCCOY, A. B., 1997, *J. chem. Phys.*, **106**, 2627.
[47] ZHANG, R., VAN DER ZANDE, W. J., BRONIKOWSKI, M. J., and ZARE, R. N., 1991, *J. chem. Phys.*, **94**, 1704.
[48] (a) ARNOLDI, D., and WOLFROM, J., 1974, *Chem. Phys. Lett.*, **24**, 234; (b) BROWN, R. D. H., GLASS, G. P., and SMITH, I. W. M., 1975, *Chem. Phys. Lett.*, **32**, 517; (c) MACDONALD, R. G., and MOORE, C. B., 1978, *J. chem. Phys.*, **68**, 513; (d) BUTLER, J. E., HUDGENS, J. W., LIN, M. C., and SMITH, G. K., 1978, *Chem. Phys. Lett.*, **58**, 216.
[49] NOBUSADA, K., TOLSTIKHIN, I., and NAKAMURA, H., 1998, *J. chem. Phys.*, **108**, 8922.
[50] LEROY, R. L., 1969, *J. phys. Chem.*, **73**, 4338.
[51] HUTSON, J. M., 1992, *J. chem. Phys.*, **96**, 4237.
[52] HERZBERG, G., 1989, *Molecular Spectra and Molecular Structure*, Vol. 1 (Malabar, Florida: Krieger).
[53] MARQUES, J. M. C., WANG, W., PARIS, A. A. C. C., and VARANDAS, A. J. C., 1996, *J. phys. Chem.*, **100**, 17513.
[54] MCCOY, A. B., LUFASO, M. W., VENEZIANI, M., ATRILL, S., and NAAMAN, R., 1998, *J. chem. Phys.*, **108**, 9651.
[55] IMURA, K., VENEZIANI, M., KASAI, T., and NAAMAN, R., 1999, *J. chem. Phys.* (in the press).